

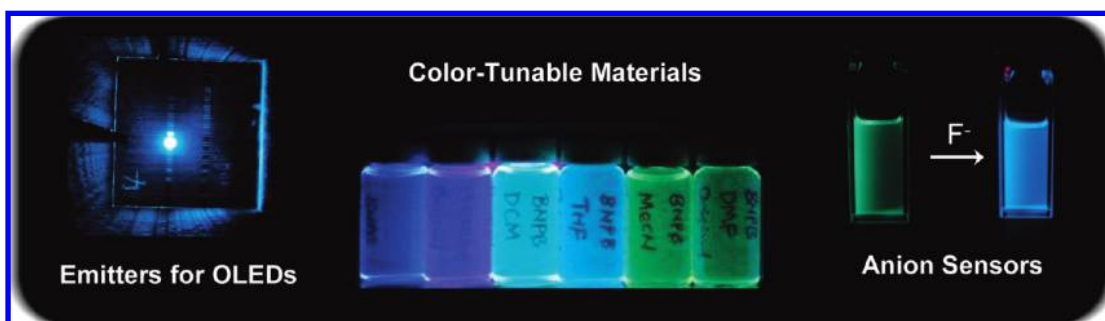
Impact of Donor–Acceptor Geometry and Metal Chelation on Photophysical Properties and Applications of Triarylboranes

ZACHARY M. HUDSON AND SUNING WANG*

Department of Chemistry, Queen's University, Kingston, Ontario K7L 3N6, Canada

RECEIVED ON MARCH 17, 2009

CON SPECTUS



Three-coordinate organoboron compounds have recently found a wide range of applications in materials chemistry as non-linear optical materials, chemical sensors, and emitters for organic light-emitting diodes (OLEDs). These compounds are excellent electron acceptors due to the empty p_π orbital on the boron center. When accompanied by electron donors such as amines, these molecules possess large electronic dipoles, which promote donor–acceptor charge-transfer upon excitation with light. Because of this, donor–acceptor triarylboranes are often highly luminescent both in the solid state and in solution.

In this Account, we describe our research to develop donor–acceptor triarylboranes as efficient blue emitters for OLEDs. Through the use of hole-transporting donor groups such as 1-naphthylphenylamines, we have prepared multifunctional triarylboranes that can act as the emissive, electron transport, or hole transport layers in OLEDs. We have also examined donor–acceptor compounds based on 2,2'-dipyridylamine or 7-azaindolyl donors, several of which have fluorescent quantum efficiencies approaching 100%.

We are also investigating the chemistry of metal-containing triarylboranes. Our studies show that the electron-deficient boryl group can greatly facilitate metal-to-ligand charge-transfer transitions and phosphorescence. In addition, electronegative linker groups such as 2,2'-bipyridine can act in synergy with metal chelation to greatly improve the electron-accepting ability and Lewis acidity of triarylboranes.

Donor–acceptor triarylboranes developed in our laboratory can also serve as a series of “switch-on” sensors for fluoride ions. When the donor and acceptor are linked by rigid naphthyl or nonrigid silane linkers, donor–acceptor conjugation is disrupted and charge transfer occurs primarily through space. The binding of fluoride ions to the boron center disrupts this charge transfer, activating alternative $\pi \rightarrow \pi^*$ transitions in the molecule and changing the emission color of the sample.

More recently, we have used these nonconjugated linkers to prepare organometallic donor–acceptor triarylboranes in which fluorescence and phosphorescence can simultaneously be observed from two different chromophores in the same molecule at ambient temperature. These dual emissive molecules remain sensitive to fluoride ions, and give synergistic singlet–triplet emission responses when titrated with F^- . Fluoride ions can also act as valuable chemical probes, providing insight into the electronic structure of this new class of optoelectronic materials.

We have demonstrated that donor–acceptor triarylboranes are promising materials in anion sensing and electroluminescent device applications. Nonetheless, despite our work and that of other research groups, there is still much to be learned about organometallic and multiply emissive triarylboron systems.

1. Introduction

Triarylboranes have recently emerged as an important class of molecules with many applications in materials sciences. The empty p_π orbital on the boron center makes these compounds excellent electron acceptors, which enables their use in such diverse fields as nonlinear optics,^{1–4} anion sensing,^{5–14} hydrogen activation and storage,^{15,16} and as emitters and electron transport materials in organic light-emitting diodes (OLEDs).^{17–21} When accompanied by an appropriate electron donor as shown in Chart 1, these compounds possess a large electrical dipole, which generates a highly polarized and emissive excited state upon excitation with light.

The aryl groups play a key role in stabilizing the radical anion generated when these compounds are used as electron transport materials in OLEDs.^{17–21} Furthermore, Yamaguchi, Gabbai, and others have demonstrated that coordination of an external donor group to the boron center can readily disrupt this extended π -conjugation, causing distinct changes in the absorption or emission spectra of the sample,^{4–14} which is the basis for their use as anion sensors. Because of the electrophilicity of three-coordinate boron, bulky *ortho*-substituted aryls (e.g., mesityl) are often employed to protect the boron center from nucleophilic attack. Such protected triarylboranes are usually very robust and stable under ambient conditions. Furthermore, such steric protection renders the Lewis acidic p orbital on the boron center inaccessible to all but the smallest nucleophiles, allowing the use of these triarylboranes as highly selective sensors for small anions such as fluoride and cyanide.^{4–14}

The use of triarylboranes in OLEDs was pioneered by Shirota and co-workers^{17–20} and led to our research on donor–acceptor triarylboranes. We were motivated primarily by the need for stable and efficient blue emitters, a key challenge in OLED research. The blue emitters developed by us represent our key contribution to this field.^{22–27} During the course of our research, we also discovered that it was possible to create and switch between multiple emission pathways in a single molecule by controlling the donor–acceptor geometry,^{28,29} thus achieving “switch-on” sensors for fluoride. We have also found that metal chelation can greatly enhance the electron-accepting ability of these materials,^{30–32} a key feature required for most applications of triarylboranes. Furthermore, we have found that triarylboron centers can dramatically enhance metal-to-ligand charge-transfer (MLCT) transitions, creating new opportunities for the development of bright phosphorescent materials.^{32,33} This Account provides an overview of our recent research on donor–acceptor triarylbo-

CHART 1

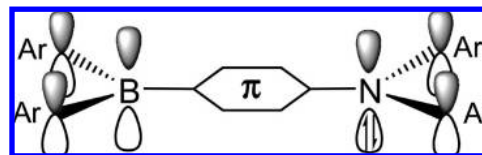
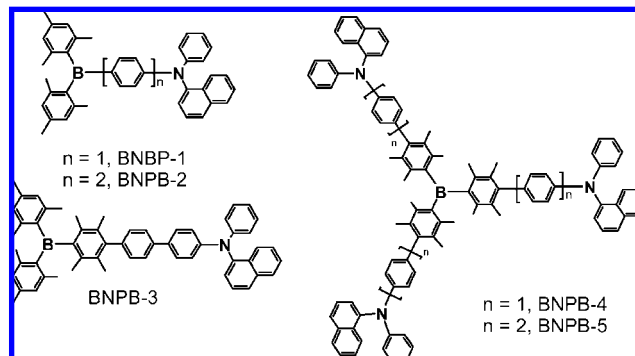


CHART 2



ranes, with emphasis on the impact of molecular shape and metal chelation on the luminescence, electron accepting ability, and Lewis acidity of this new class of materials. Synthetic methods for compounds in this Account can be found in the original publications.

2. Conjugated Donor–Acceptor Systems

2.1. The BNPB System: Efficient Blue Emitters for OLEDs. The (1-naphthyl)phenylamino group NPB is part of the widely used “NPB” hole transport material *N,N'*-di(naphthalene-1-yl)-*N,N'*-diphenylbenzidine, commonly used in OLEDs. Hence, this donor group was chosen in order to achieve compounds that could function as emissive, electron transport, or hole transport materials in electroluminescent (EL) devices. Five triarylboranes, BNPB-1 to BNPB-5, were obtained and are shown in Chart 2.^{22–24}

All five molecules show reversible oxidation and reduction peaks in their CV diagrams, reminiscent of the bipolar triarylboranes reported by Shirota et al.¹⁹ The LUMO levels of BNPB-1 and 2 (−2.42 and −2.44 eV) are considerably lower than those of BNPB-3–5 (−2.13 eV) due to the poor conjugation of the duryl-containing molecules. This reduced conjugation also greatly lowers the quantum efficiency of BNPB-3–5 (22%–27%) relative to BNPB-1 and -2 (62%–82%), making the latter better candidates for applications as emitters in OLEDs. However, the branching in BNPB-4 and -5 makes these compounds more thermally stable (glass transition temperature, T_g , 171–173 °C) than their linear counterparts (T_g 106–110 °C).²³

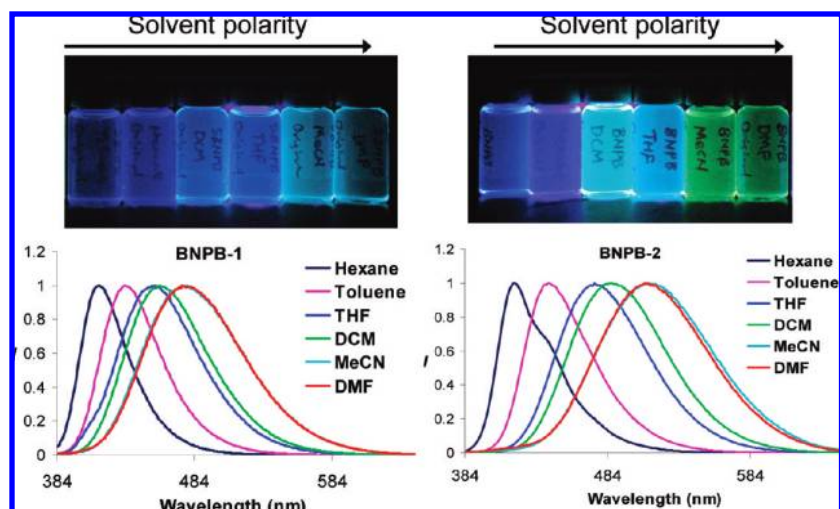


FIGURE 1. Photographs and emission spectra of BNPB-1 and BNPB-2 in various solvents.

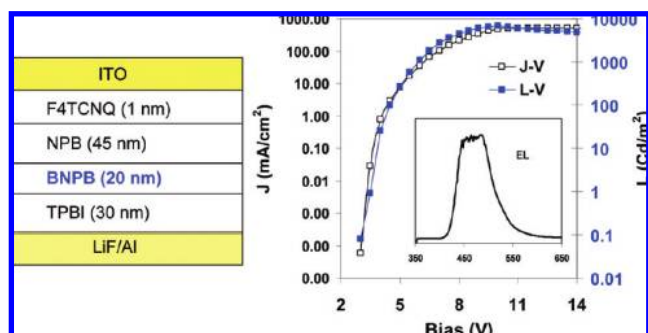


FIGURE 2. The EL device structure (left) and L – J – V characteristics and EL spectrum (right) of the BNPB-based device.

All five molecules display highly solvent-dependent emission, characteristic of donor–acceptor charge transfer and a highly polarized excited state, as shown by the spectra of BNPB-1 and -2 in various solvents (Figure 1).^{22,23}

The performance of BNPB-2 as an emitter in OLEDs was investigated because of its blue emission (451 nm) and high quantum efficiency in the solid state (33%). Simple double-layer EL devices with structures of indium tin oxide (ITO)/BNPB-2/tris(8-hydroxyquinolino)aluminium (Alq₃)/LiF/Al and ITO/NPB/BNPB-2/Ag established that BNPB-2 can indeed function as either a hole transport or a bifunctional electron transport blue-emitting material.²² More sophisticated device structures led to bright EL devices that are among the most efficient blue OLEDs reported in the literature.²⁴ An example is shown in Figure 2, with the structure of ITO/F₄TCNQ/NPB/BNPB-2/TPBI/LiF/Al where F₄TCNQ (2,3,5,6-tetrafluoro-7,7,8,8-tetracyanoquinodimethane) is the hole injection layer, NPB the hole-transport layer, BNPB-2 the emitter, and TPBI (1,3,5-tris(2-*N*-phenylbenzimidazolyl)benzene) the electron-transport layer. This device has a brightness of ~7000 cd/m² at 10 V and current and power efficiency as high as 3.5 cd/A and 2.5 lm/W, respectively, at 200 cd/m² (4.5 V). The large star-shaped mol-

ecule BNPB-5 has been found to be an effective hole-transport and hole-injection material in OLEDs.²³

Inspired by the earlier fluoride sensing work of Yamaguchi and Gabbai,^{5–10} we examined the response of BNPB-1 and -2 toward fluoride. UV–vis, fluorescence, and ¹H or ¹⁹F NMR titration experiments showed that both molecules bind selectively to fluorides with little affinity toward chloride or bromide, consistent with the steric protection of the boron center by the mesityls.^{28,29} This is in fact true for all triarylboranes presented in this Account. The N → B charge-transfer band in the absorption spectra of both compounds loses intensity with a corresponding quenching of the fluorescent peak as fluoride ions bind to the boron center (Figure 3). Because of the quenching response, this group of compounds can be described as “switch-off” sensors for fluorides.

2.2. The DPA and AZAIN Systems: Metal Ion-Binding Blue Emitters. Our earlier work on 7-azaindoly (AZAIN) and 2,2'-dipyridylamino (DPA) derivatives established that these chromophores are very efficient blue emitters when attached to ions such as Zn(II), B(III), or Al(III).^{34–37} Hence, we developed new triarylboranes that contain either DPA or AZAIN,^{25,26} shown in Chart 3. The crystal structures of BDPA-4, BDPA-7, and BAZAIN-3 determined by X-ray crystallographic analysis (Figure 4) show that the arylboron unit is completely noncoplanar with the DPA substituent but approximately coplanar with the 7-azaindoly group.²⁶ The large branched molecule BDPA-7 forms an interlocked pair in the crystal lattice.²⁶

This class of molecules in general possess high melting points (141–260 °C), and in some cases, a high T_g (e.g., BDPA-2, T_g = 132 °C). A reversible reduction peak for most members in this group was observed by cyclic voltammetry.²⁶ All molecules in this group are blue emitters, with consider-

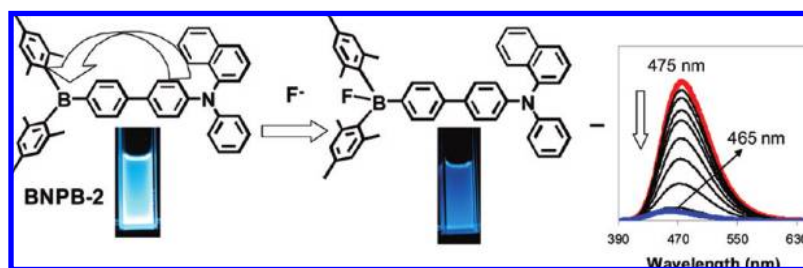
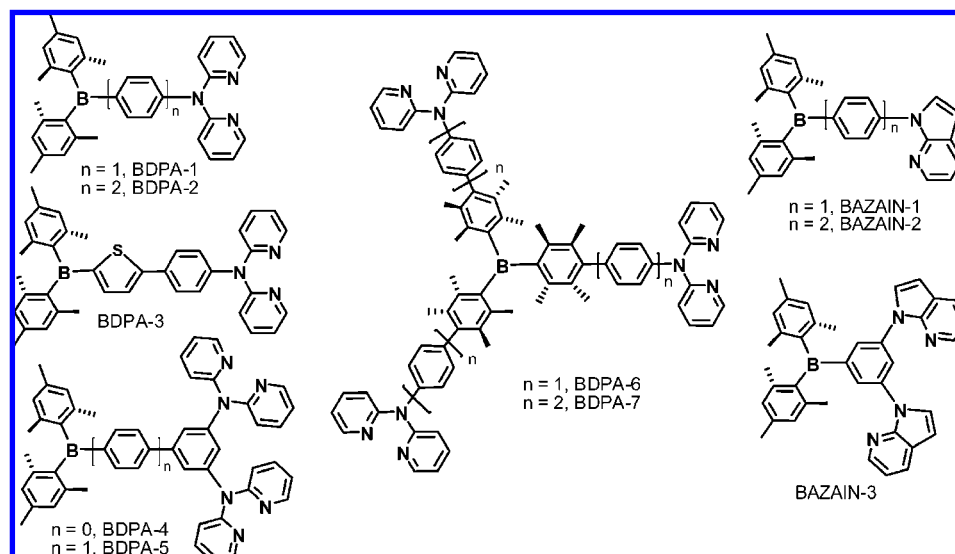


FIGURE 3. Photographs and the emission spectral change of BNPB-2 before and after the addition of TBAF in CH_2Cl_2 (all titration spectra were recorded at $\sim 1.0 \times 10^{-5}$ M).

CHART 3



able variation in emission energy and efficiency. BDPA-1 and BDPA-3, in particular, are highly efficient emitters with quantum efficiencies approaching 100%.^{25,26} Compared with the corresponding DPA analogues ($\lambda_{\text{em}} = 405\text{--}465$ nm), the

AZAIN functionalized molecules emit at much shorter wavelengths ($\lambda_{\text{em}} = 381\text{--}417$ nm) in solution and the solid state. Nonetheless, solvent-dependent fluorescence measurements and DFT calculations established that in both cases, the emission is due to donor–acceptor charge transfer. The *para*-substituted linear molecules were found to have the highest quantum efficiencies of both the DPA and AZAIN derivatives, suggesting that intramolecular charge transfer is most favored in this geometry. The thienyl linker in BDPA-3 was found to enhance the emission efficiency and lower the emission energy of BDPA-3 (465 nm, 100%) compared with the phenyl analogue BDPA-2 (449 nm, 63%) due to improved donor–acceptor π -conjugation.

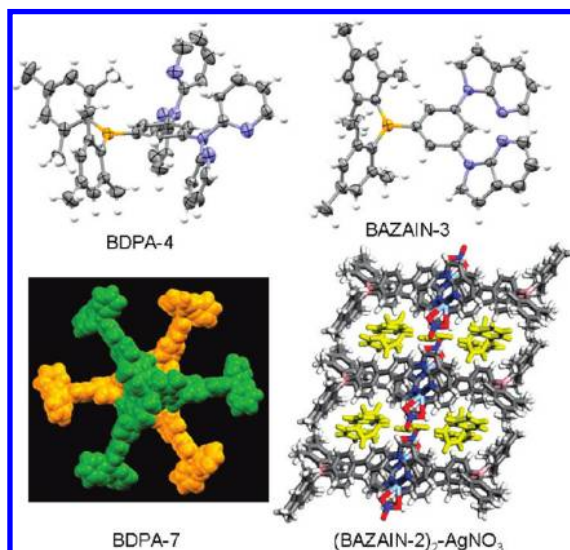
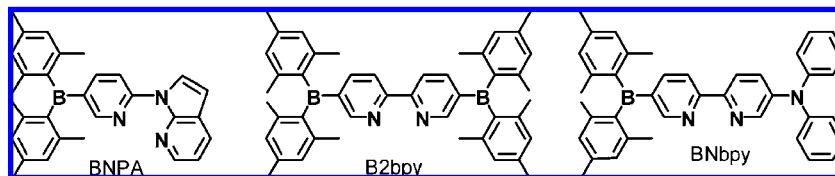


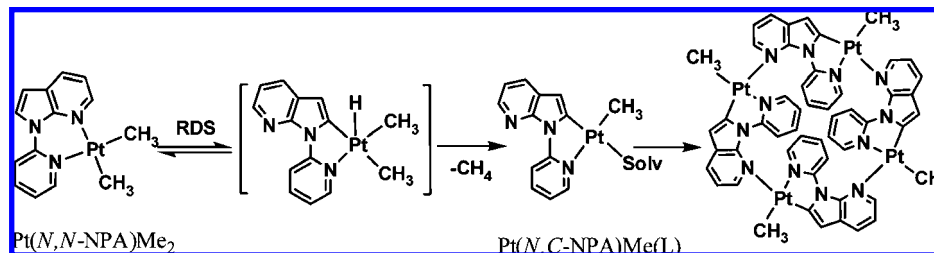
FIGURE 4. Crystal structure of BDPA-4, BAZAIN-3, BDPA-7, and $(\text{BAZAIN-2})_2\text{-AgNO}_3$ showing benzene (yellow) inclusion in the lattice.

Binding by metal ions such as Zn(II) and Ag(I) diminishes the charge-transfer emission somewhat, due to mostly electron donation to the metal ion. In the case of Ag(I), intersystem crossing to the less emissive triplet state could also contribute to this reduced intensity. Interestingly, however, the metal complexes of this group of molecules were found to have the tendency to form porous crystal lattices. An example is the crystal lattice of the $(\text{BAZAIN-2})_2\text{-AgNO}_3$ complex

CHART 4



SCHEME 1



shown in Figure 4, which hosts benzene molecules selectively, demonstrating the potential of such a triarylborane–metal hybrid framework for selective hosting/sensing of organic molecules.^{25,26}

Preliminary evaluation on the performance of BDPA-2 and -3 in OLEDs was conducted. Blue EL devices with moderate brightness were achieved with simple device structures of ITO/NPB/HBL/BDPA-2(3)/LiF/Al, where HBL is a hole blocking layer, demonstrating that the BDPA molecules can act as bifunctional blue emitters in OLEDs.²⁶ Optimization of the device structures for BDPA-2 and BDPA-3 has not yet been performed.

2.3. Heterocyclic Systems: Increasing Donor–Acceptor Conjugation. Although the molecules in section 2.2 are capable of binding to metal ions, the donor–acceptor conjugation and electronic communication between the metal center and the B center are weak. In search of strongly conjugated donor–acceptor systems that also promote strong electronic communication between the boron and the metal center, we synthesized triarylboranes in which the boron center is attached directly to an electronegative *N*-heterocycle. With this approach, two new classes of triarylboranes based on 2,2'-bipyridine (bpy) and *N*-(2'-pyridyl)-7-azaindole (NPA) have been developed by our group (Chart 4).

BNPA was developed based on our recent discovery that NPA reacts with Pt(II) to form an unstable six-membered N,N-

chelate ring that promotes a facile “roll-over” cyclometalation, forming a more stable, planar five-membered N,C-chelate ring³⁸ as shown in Scheme 1. When functionalized with three-coordinate boron, this architecture would thus provide us with a versatile framework for the investigation of metal-containing triarylboranes. B2bpy and BNbpy were investigated^{30,31} because of the excellent chelating ability of 2,2'-bipyridine. The structures of BNPA and B2bpy determined by X-ray diffraction are shown in Figure 5. In both cases, the intramolecular hydrogen bond between the N atom of the *N*-heterocycle and the adjacent *ortho* protons promotes coplanarity of the heterocyclic rings and thus conjugation with the B center.

As a consequence of the enhanced π conjugation, BNPA, B2bpy, and BNbpy are stable toward reduction and display reversible reduction peaks that are considerably more positive than those observed in the BNPB or BDPA series. The B2bpy molecule has two fully reversible reduction peaks at -1.69 and -2.04 V (vs $\text{FcCp}_2^{0/+}$, Figure 11), while BNbpy has a single reduction peak at -1.99 V, corresponding to LUMO energies of -3.11 and -2.81 eV, respectively. Compared with the biphenyl linker (BMe_2 –biphenyl– BMe_2 ,³⁹ LUMO ≈ -2.84 eV), the bpy linker is clearly more effective in lowering the LUMO level due to its greater electronegativity. The deep LUMO level makes these molecules good candidates as electron-transport materials in OLEDs.

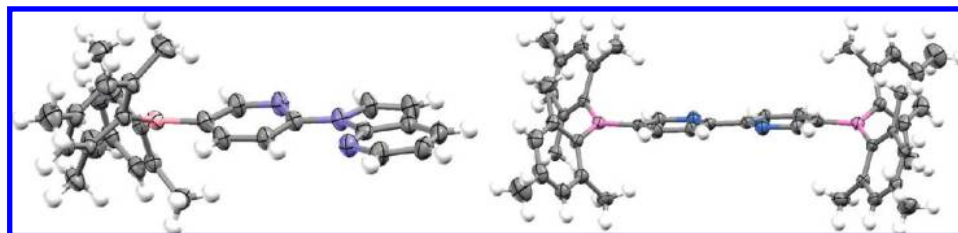


FIGURE 5. Crystal structures of BNPA and B2bpy.

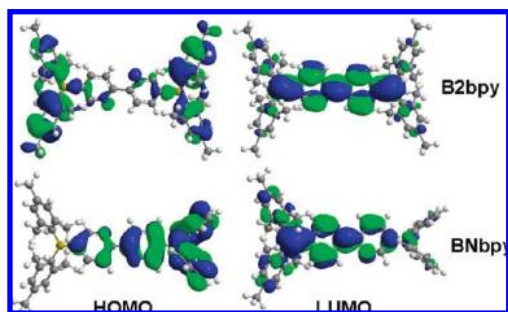


FIGURE 6. HOMO and LUMO diagrams of B2bpy and BNbpy.

Although all three molecules are luminescent, B2bpy has a very low quantum efficiency (1%) while BNPA and BNbpy have quantum efficiencies of 25% and 95%, respectively. The nature of the lowest energy transitions in the three molecules was determined to be NPA \rightarrow B (BNPA), NPh₂ \rightarrow B-py (BNbpy), and mesityl \rightarrow B-bipy-B (B2bpy) by TD-DFT calculations (Figure 6). Compared with BNBP-2, a biphenyl analogue of BNbpy, the emission energy of BNbpy is considerably red-shifted and the emission spectrum has a much greater dependence on solvent polarity, consistent with its smaller HOMO–LUMO gap and enhanced donor–acceptor conjugation.

BNPA, B2bpy, and BNbpy each respond to fluoride in both absorption and emission modes.^{30–33} In absorption mode, the addition of fluoride diminishes the charge-transfer transition band for all three compounds. Consistent with the strong electron-accepting ability, the binding constant of BNbpy with fluoride ($2.5 \times 10^6 \text{ M}^{-1}$) is considerably larger than that of BNBP-2 ($1.4 \times 10^5 \text{ M}^{-1}$) in CH₂Cl₂, while a clear stepwise binding by two fluoride ions is evident in the UV–vis spectrum of B2bpy (Figure 7) with a very large binding constant ($K_1 \geq 10^8 \text{ M}^{-1}$).

In fluorescent mode, both BNPA and B2bpy undergo quenching with fluoride, while BNbpy displays an unusual “turn-on” response that is independent of solvent or excitation energy, as shown in Figure 8. This is likely due to the presence of a low-energy $\pi \rightarrow \pi^*$ emission pathway originating on the donor-linker π system, made possible by the highly coplanar bipyridine bridge. Thus, “turn-on” fluorescent sensors for fluoride can be achieved in conjugated donor–acceptor organoboron compounds if a sufficiently conjugated and electronegative linker is employed.

2.4. The BNPA System: Enhancing Metal-to-Ligand Charge Transfer Phosphorescence. The impact of triarylboranes on MLCT phosphorescence was first examined using three complexes, Pt(BNPA)Ph₂, Pt(BNPA)Cl₂, and [Cu(BNPA)(PPh₃)₂]BF₄ (Cu-BNPA), shown in Scheme 2.³² The choice of Pt(II) and Cu(I) was based on the fact that these metal ions are known to facilitate diimine-based MLCT phosphorescence. The

Pt(BNPA)Ph₂ complex undergoes cyclometalation in solution to form the N,C-chelate complex Pt-N,C-BNPA either slowly at room temperature or rapidly at 60 °C, which can then be trapped by various donors, such as SMe₂.³³

Pt(BNPA)Ph₂ shows bright yellow phosphorescence at ambient temperature in CH₂Cl₂ (543 nm, $\Phi_p = 0.4\%$, $\tau = 25.0 \mu\text{s}$) and in the solid state (519 nm, $\Phi_p = 10\%$, $\tau = 10.9 \mu\text{s}$), characterized by a broad MLCT transition from the Pt center to the boron- p_π containing LUMO of the ligand. Consistent with the MLCT assignment, the Pt(BNPA)Cl₂ complex is not luminescent. The electron-deficient boron was found to be instrumental in facilitating the MLCT emission, as the boron-free analogue Pt(NPA)Ph₂ exhibits only a very weak, structured emission band similar to that of free NPA (487 nm, $\tau = 18.5 \mu\text{s}$). Furthermore, addition of F[−] to the solution of Pt(BNPA)Ph₂ caused quenching of the MLCT band, with appearance of the NPA-based structured band at 497 nm ($\tau = 10.9 \mu\text{s}$) as a result of blocking the boron p_π orbital (Figure 9). The luminescence of Pt(BNPA)Ph₂ is highly sensitive to oxygen, requiring less than 2% O₂ to quench $\sim 90\%$ of the emission, which can be fully restored using nitrogen, making it a potentially useful oxygen-sensing reagent.

As shown by the crystal structures in Figure 10, Pt(BNPA)Ph₂ contains a highly strained six-membered ring that is puckered out of plane, with a large torsion angle between the py and 7-azaindolyl rings. In contrast, the Pt-N,C-BNPA compound contains a more stable, planar five-membered chelate ring, the formation of which provides the driving force for the C–H bond activation. Consequently, Pt-N,C-BNPA is a much more efficient phosphorescent chromophore than its N,N-chelating counterpart with a quantum efficiency ~ 8 times greater than that of Pt(BNPA)Ph₂ (535 nm, $11.9 \mu\text{s}$, $\Phi_p = 3.2\%$).³³

The MLCT emission band of Pt-N,C-BNPA changes with fluoride in the same manner as the N,N-chelate compound, switching from yellow MLCT to green NPA-based phosphorescence at $\lambda_{\text{max}} = 480 \text{ nm}$. We have thus demonstrated that the MLCT phosphorescence of the Pt(II) boron-containing compounds can be enhanced by careful control of the chelate mode and binding geometry around the metal center.

The Cu-BNPA complex also exhibits bright MLCT-based phosphorescence in CH₂Cl₂ solution (Figure 9) with a 10-fold increase in quantum efficiency ($\Phi_p = 4\%$) over Pt(BNPA)Ph₂. More remarkably, this complex was found to have the highest solid-state quantum efficiency of any known Cu(I) compounds ($\Phi_p = 88\%$),³² and efforts are underway in our laboratory to make use of this material in OLEDs.

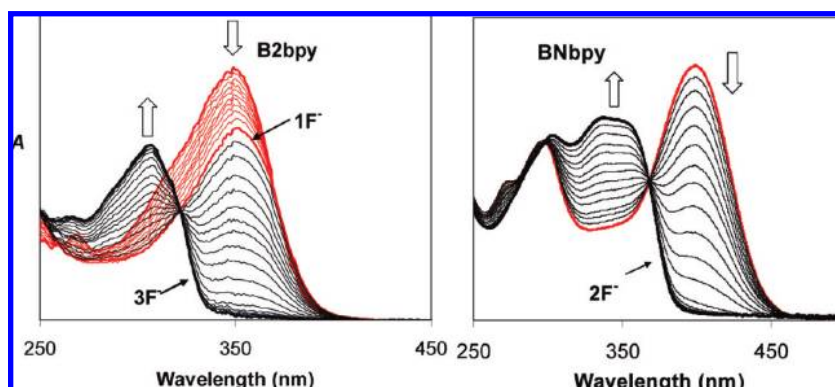


FIGURE 7. Absorption spectral change of B2bpy and BNbpy with TBAF in CH_2Cl_2 .

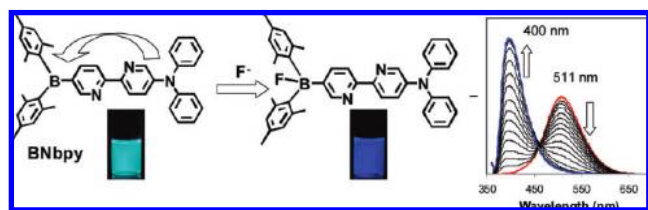
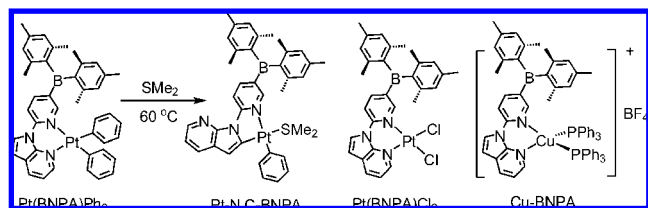


FIGURE 8. Photographs and emission spectral change of BNbpy before and after the addition of TBAF in CH_2Cl_2 .

SCHEME 2



2.5. The Bipy System: Increasing Electron-Accepting Ability. B2bpy and BNbpy are effective chelate ligands, from which we synthesized several Pt(II) and Cu(I) complexes shown in Chart 5. The structures of $\text{Pt}(\text{B2bpy})\text{Ph}_2$ and $\text{Pt}(\text{B2bpy})\text{Cl}_2$ determined by X-ray diffraction analyses are shown in Figure 11.

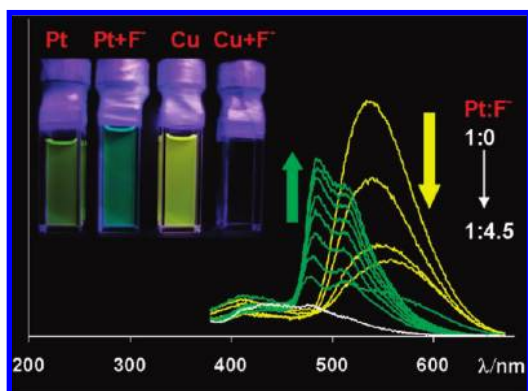


FIGURE 9. Phosphorescent spectral change of $\text{Pt}(\text{BNPA})\text{Ph}_2$ with F^- in CH_2Cl_2 . The inset shows photographs of $\text{Pt}(\text{BNPA})\text{Ph}_2$ and $[\text{Cu}(\text{BNPA})(\text{PPh}_3)_2]\text{BF}_4$ before and after F^- .

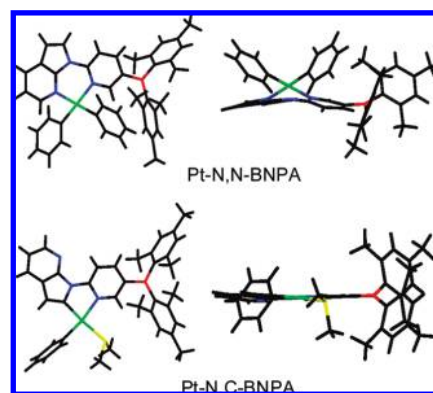
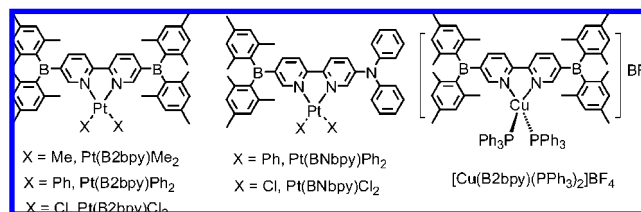


FIGURE 10. Top and side views of crystal structures of $\text{Pt}(\text{BNPA})\text{Ph}_2$ and $\text{Pt}(\text{N,C-BNPA})\text{Ph}_2$.

CHART 5



Like the free ligand, the B2bpy complexes^{30,31} display fully reversible reduction peaks but at much more positive potentials (-1.17 to -1.38 V vs Fc/Fc^+) than the free ligands (Figure 11), attributed to the enhanced π -conjugation via metal chelation and σ -donation from the nitrogen atoms to the metal center. $\text{Pt}(\text{B2bpy})\text{Cl}_2$ has the most positive reduction potential (-1.17 V), consistent with the weaker *trans* effect of the chloride, comparable to that of $\text{B}(\text{C}_6\text{F}_5)_3$. Another important feature of the B2bpy complexes is their intense, ancillary ligand-dependent color due to a low-energy MLCT band in the absorption spectra (e.g., $\text{Pt}(\text{B2bpy})\text{Me}_2$, dark green; $\text{Pt}(\text{B2bpy})\text{Ph}_2$, dark red; $\text{Pt}(\text{B2bpy})\text{Cl}_2$, bright yellow in toluene). Analogous boron-free bipy complexes are either light yellow or yellow, demonstrating again the key role of the boron center in promoting the MLCT transition.

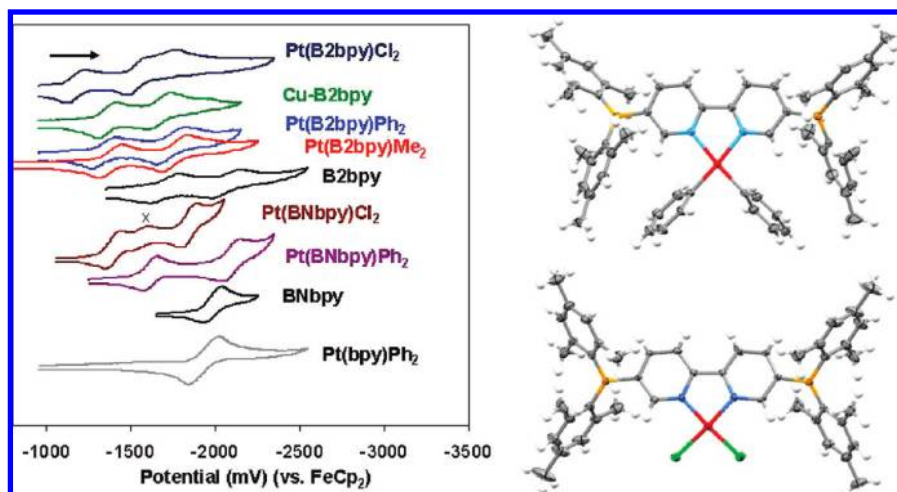


FIGURE 11. CV diagrams (left) of B2bpy, BNbp, their metal complexes, and Pt(bpy)Ph₂ and crystal structures (right) of Pt(B2bpy)Ph₂ and Pt(B2bpy)Cl₂.

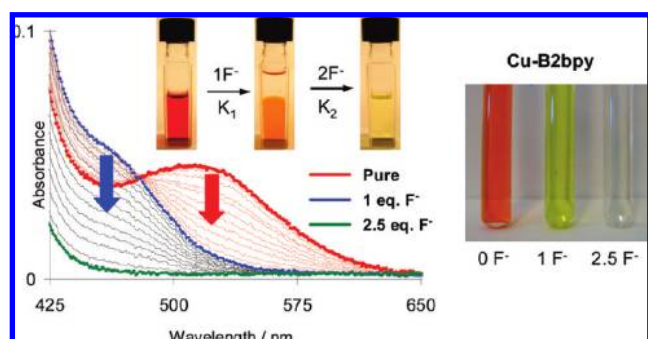


FIGURE 12. UV–vis titration diagram of Pt(B2bpy)Ph₂ (left) and photographs showing the color change of Pt(B2bpy)Ph₂ and [Cu(B2bpy)(PPh₃)₂]BF₄ (right) with F[−] in CH₂Cl₂.

Both the Cu(I) and Pt(II) complexes of B2bpy were found to bind very strongly to fluoride. For example, titration of a CH₂Cl₂ solution of Pt(B2bpy)Ph₂ with tetra-*n*-butylammonium fluoride (TBAF) gives a sequential color change from red to orange as 1 equiv of F[−] is added and then from orange to yellow with addition of a second F[−], with binding constants of $\geq 10^9$ and 10^6 M^{−1}, respectively, due to the sequential quenching of the MLCT band (Figure 12). Consistent with the large binding constant, Pt(B2bpy)Ph₂ and [Cu(B2bpy)(PPh₃)₂]⁺ are capable of binding to 1 equiv of fluoride even in the presence of methanol or water, a significant finding given the high hydrogen bond enthalpy of the fluoride ion. Hence, complexes of B2bpy were shown to be not only strong electron acceptors but also highly sensitive visual colorimetric sensors for fluoride in organic media.

Complexes of BNbp also showed significantly higher reduction potentials than the free ligand. However, unlike the nonemissive B2bpy complexes, BNbp complexes are luminescent in solution at ambient temperature, displaying orange to red phosphorescence under air ($\lambda_{\text{max}} = 565$ nm, $\tau = 6.80$

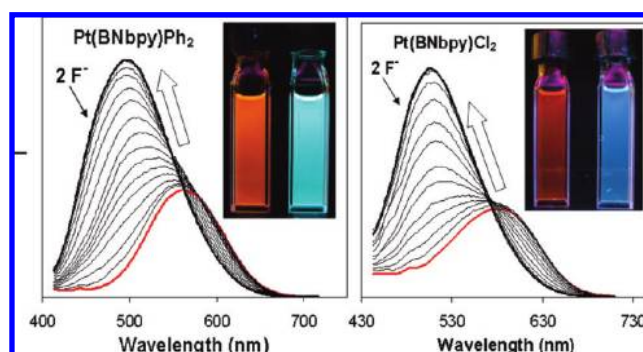


FIGURE 13. Phosphorescent titration diagrams of Pt(BNbp)Ph₂ and Pt(BNbp)Cl₂ by TBAF in CH₂Cl₂ under air.

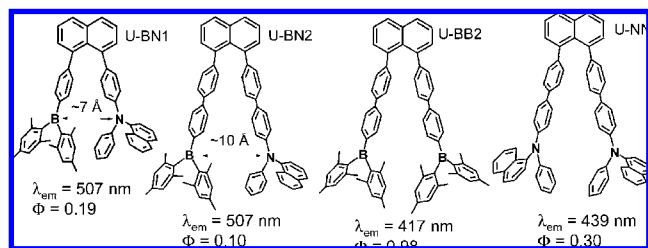
μs for Pt(BNbp)Ph₂ and 591 nm, $\tau = 7.70$ μs for Pt(BNbp)Cl₂). In each case, DFT calculations indicated this transition to be MLCT in nature, though based on the absorption spectra they likely involve contributions from intraligand Ph₂N → B charge transfer as well.³¹

Interestingly, luminescent titrations of either Pt(BNbp)Ph₂ or Pt(BNbp)Cl₂ by fluoride under air gave a very dramatic color change, as the emission in each case was switched from red-orange to blue-green with a large increase in emission intensity (Figure 13). This phosphorescent response is reminiscent of the fluorescent “turn-on” response of free BNbp and attributable to the blocking of the N → B/MLCT transition with activation of a $\pi \rightarrow \pi^*$ transition. This demonstrates that by incorporating an internal donor–acceptor system into the chelate ligand, phosphorescent “turn-on” sensors for fluoride may be achieved.

3. Nonconjugated Systems

In an effort to understand donor–acceptor charge transfer in nonconjugated triarylboron systems, we investigated several

CHART 6



U-shaped and V-shaped molecules, namely the U-BN, Si-BNPB, and SiBNSA systems in which the donor (N(1-naph)Ph or NPA) and the BMes_2 acceptor are separated by either a rigid naphthyl or nonrigid silane linker.

3.1. The U-BN System: Through-Space Charge Transfer. Two donor–acceptor molecules, U-BN1 and U-BN2, as well as the acceptor-only and donor-only analogues U-BB1, U-BB2, and U-NN (Chart 6) were prepared and examined.^{28,29} Due to the steric demands of the linker, the two chromophores adopt a nonconjugated conformation, and thus each should possess frontier orbitals that resemble those of the parent chromophores. This rigid linker allows these chromophores to communicate electronically by a weak charge transfer through space. Binding of fluoride to the boron center can then block the charge-transfer transition, leaving the lowest energy transition of the donor group as the only source of emission.

In solution, both U-BN1 and U-BN2 display a broad fluorescent peak at 507 nm in CH_2Cl_2 with low quantum efficiency ($\Phi_f = 19\%$, 10% for U-BN1 and U-BN2, respectively) and a strong dependence on solvent polarity, both characteristic of charge-transfer emission and further confirmed by DFT calculations. However, this unique through-space charge transfer is best demonstrated by comparison with U-BB1, U-BB2, and U-NN, which all show blue-shifted emission with considerably higher quantum efficiencies than their donor–acceptor analogues (Chart 6).²⁹

For many applications of luminescent materials, it is desirable to have a high quantum efficiency, but this is not always necessary for sensor applications as demonstrated by U-BN1 and U-BN2. When titrated with TBAF in CH_2Cl_2 , the charge-transfer band in both compounds is quenched, with the appearance of a much brighter $\pi \rightarrow \pi^*$ emission band at 460 nm for U-BN1 and 453 nm for U-BN2. Addition of F^- thus switches the emission color of the solution from green to blue (Figure 14). In contrast, when U-BB1 and U-BB2 are titrated with TBAF, the emission is simply quenched, establishing unequivocally that the activated emission originates on the donor group (Scheme 3). However, the U-shaped U-BN1 and U-BN2 have been found to have much lower binding con-

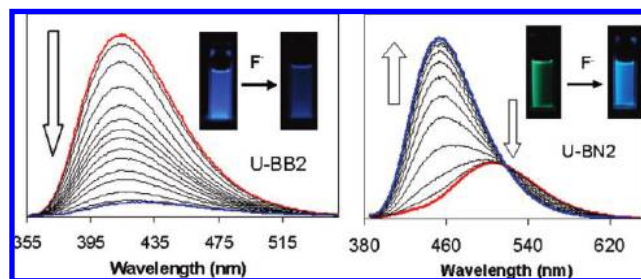
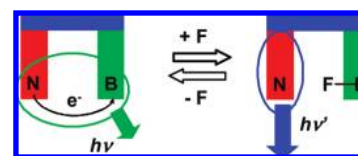


FIGURE 14. Fluorescent titration diagrams of U-BB2 and U-BN2 by TBAF in CH_2Cl_2 .

SCHEME 3



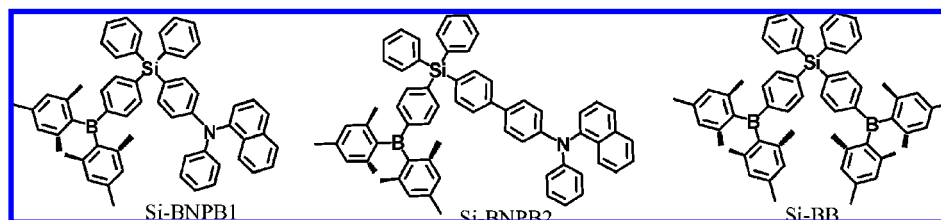
stants with fluoride ($K = 1.4 \times 10^4$ and $4.0 \times 10^4 \text{ M}^{-1}$, respectively, in CH_2Cl_2) than the conjugated molecule BNPB-2 ($K = 1.2 \times 10^5 \text{ M}^{-1}$ in CH_2Cl_2), despite their similar reduction potentials. This can be attributed to the steric congestion in the U-shaped molecules.²⁷

3.2. The SiBNPB System: Optimizing “Switch-On” Fluoride Sensing. After studying the U-BN system, we investigated nonconjugated donor–acceptor systems based on flexible tetrahedral silanes. Compounds Si-BNPB1 and -2 were prepared in order to determine the effects of donor–acceptor separation distance on the charge transfer transition.²⁹ The acceptor-only molecule Si-BB was also synthesized for comparison (Chart 7).²⁷

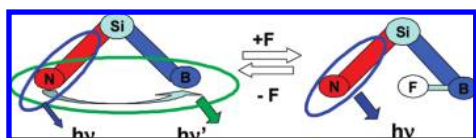
Si-BNPB1 exhibits through-space charge-transfer emission similar to U-BN1 and U-BN2. Si-BNPB2, however, showed this charge transfer only as a weak shoulder band to a much stronger $\pi \rightarrow \pi^*$ transition, the position of which was relatively invariant with solvent polarity. Si-BNPB1 also shows the $\pi \rightarrow \pi^*$ transition as a shoulder band to the charge transfer, giving these compounds increased overall quantum efficiencies (27–36%) relative to the U-BN system. DFT calculations gave donor–acceptor distances for Si-BNPB1 and -2 of 10.1 and 13.9 Å, respectively, supporting that increasing the donor–acceptor separation distance weakens the charge-transfer interaction while strengthening $\pi \rightarrow \pi^*$ emission. This separation distance can thus be used to control the relative strengths of these competing emission pathways in nonconjugated triarylboranes.

Like the U-BN system, Si-BNPB1 and -2 act as “switch-on” sensors for fluoride, changing emission color from green to blue in the presence of F^- (Figure 15), with a large increase in emission intensity. However, these flexibly linked molecules

CHART 7



SCHEME 4



bind to fluoride much more strongly than their rigid naphthyl counterparts, with binding constants similar to that of BNPB-2. As expected, the acceptor-only molecule Si-BB experiences fluorescent quenching only with the addition of fluoride. Hence, the V-shaped donor–acceptor molecules make excellent “turn-on” sensors for F^- in organic media. The dual emissive pathways exploited for this purpose are illustrated in Scheme 4. These studies have thus established that by controlling the donor–acceptor geometries in triarylboranes, “switch-on” sensors for fluoride can be achieved.

3.3. The Si-BNPA System: Singlet–Triplet Dual Emission. We recently synthesized the V-shaped molecule Si-BNPA, which includes a triarylboron center and an NPA chelate linked together by a tetraphenylsilane. This molecule takes advantage of the optimal geometry for “switch-on” fluoride sensing while allowing us to study the impact of the N,N-NPA and N,C-NPA chelate modes in a nonconjugated geometry.³³

Si-BNPA is fluorescent in the solid state and solution at ambient temperature (405 nm, $\Phi_f = 12\%$). Addition of F^- causes quenching of this peak with the appearance of a new, blue-shifted peak at 362 nm (Figure 16). Based on the energies and solvent dependence of these transitions, they have been assigned to Mes \rightarrow B charge transfer and NPA-based $\pi \rightarrow \pi^*$ emission, respectively (Scheme 5). The “turn-on”

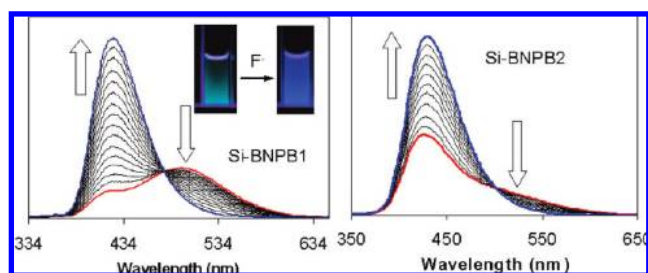


FIGURE 15. Fluorescent titration spectra of Si-BNPB1 and Si-BNPB-2 with TBAF in CH_2Cl_2 .

response of Si-BNPA toward F^- is caused by the highly emissive NPA chromophore, which shares a common excitation wavelength with the BMe_2 group.

At 77 K, Si-BNPA emits white light both in the solid state and in solution under UV irradiation, which visibly persists as green emission for ~ 3 s once the irradiation source is switched off (Figure 17). This green emission shows a band structure similar to that of frozen NPA solution, with a long decay lifetime (2.2 s). Together with the fluorescence (359 nm, $\tau = 2.0$ ns) from the BMe_2 group, this singlet–triplet dual emission gives rise to white light. The singlet and triplet emission peaks share the same excitation energy, which is responsible for the unusual singlet–triplet dual emission. To achieve ambient temperature singlet–triplet dual emission, we then explored Si-BNPA metal complexes.

Reaction of Si-BNPA with $[PtPh_2(SMe_2)]_n$ at -10 °C gave Pt-N,Si-BNPA as the kinetic product (Scheme 6), which shows weak green phosphorescence in the solid state, but in solution, the emission spectrum is characterized by two well-resolved bands. The singlet Mes \rightarrow B 1CT peak observed in the

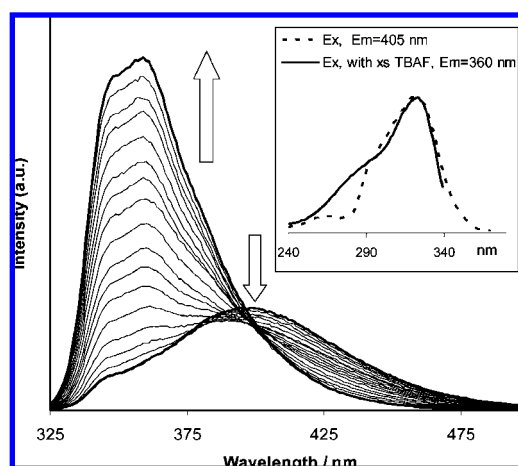
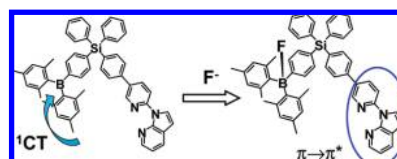


FIGURE 16. Fluorescent spectral change of Si-BNPA with TBAF in CH_2Cl_2 .

SCHEME 5



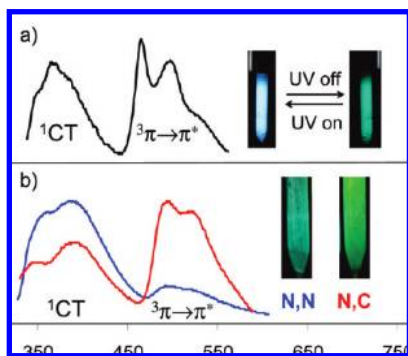
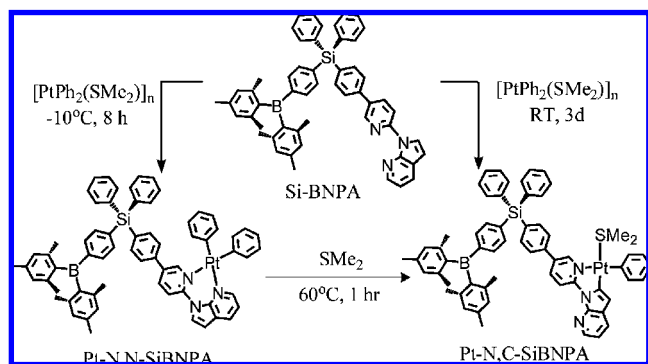


FIGURE 17. (a) Emission spectrum of Si-BNPA at 77 K in CH_2Cl_2 . (b) The normalized emission spectra of Pt-N,N-SiBNPA, and Pt-N,C-SiBNPA at ambient temperature in CH_2Cl_2 .

SCHEME 6



free ligand is preserved in the Pt complex, albeit with lower quantum efficiency (399 nm, $\Phi_{\text{F}} = 2\%$). In addition, a structured phosphorescent band at 494 nm ($\Phi_{\text{P}} = 0.7\%$, $\tau = 12.2 \mu\text{s}$), as a result of an NPA-based $^3\pi \rightarrow \pi^*$ transition, is also observed. Thus, metal chelation enhanced the emission from the triplet state of the free ligand sufficiently to allow observation of singlet–triplet dual emission at ambient temperature.

Consistent with the BNPA system, the Pt-N,C-SiBNPA complex has a much greater phosphorescent emission efficiency (495 nm, $\Phi_{\text{P}} = 2.5\%$, $\tau = 12.1 \mu\text{s}$) than the N,N-complex, such that the dual emission is now dominated by the phosphorescent band (Figure 17). The fluorescent quantum efficiency, however, remains unchanged, further supporting its boron-centered origin. One surprising finding was the response of Pt-N,C-SiBNPA to fluoride.³³ Unlike the N,N-chelate complex, which responds weakly to fluorides, addition of ~ 2 equiv of TBAF to a CH_2Cl_2 solution of Pt-N,C-SiBNPA causes a huge increase in phosphorescent intensity (Figure 18), accompanied by a switch to lower wavelength of the singlet peak, giving a synergistic, dual-emissive response to F^- . Blocking of the boron center likely makes the NPA-centered $^1\pi \rightarrow \pi^*$ transition the next lowest energy transition in the molecule, thus enhancing its population, which in turn increases the population of $^3\pi \rightarrow \pi^*$ due to efficient intersystem crossing

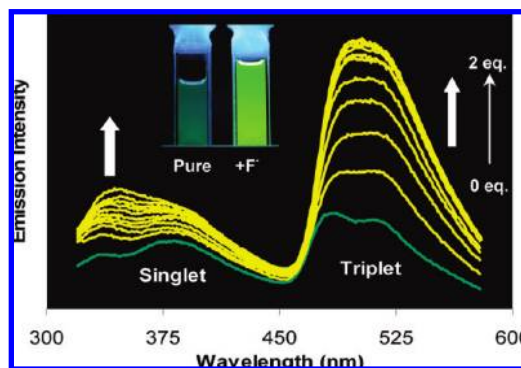


FIGURE 18. Emission spectral change of Pt-N,C-SiBNPA with TBAF at ambient temperature.

promoted by the Pt(II) atom. This demonstrates the feasibility of using spatially separated chromophores that share a common excitation energy to achieve singlet–triplet dual emission in a single molecule and the strategy of switching/enhancing singlet and triplet emission selectively by using metal chelate and fluoride ions.

4. Conclusion and Outlook

We have demonstrated that donor–acceptor triarylboranes are promising materials in anion sensing and electroluminescent device applications. We have shown that the electron-accepting ability of these molecules can be increased by incorporating electronegative linkers and metal ions into the donor–acceptor π -conjugated backbone. Furthermore, with careful control of molecular geometry, a wide range of fluorescent and phosphorescent materials with one or more emission bands can be achieved. The combination of the Lewis acidity/electron-transporting properties of triarylboranes with the rich photochemical and photophysical properties of transition metals will certainly lead to many new applications and avenues for research. Besides our work, several groups have recently shown that triarylboron-functionalized metal complexes can be used in OLEDs and sensing.^{40–44} Nonetheless, this field remains largely unexplored. There is still much to be learned about dual- and multiply-emissive triarylboron systems. Therefore, we will continue our efforts in understanding the relationship between molecular geometry, metal chelation, and luminescence in donor–acceptor triarylboron systems.

The authors would like to thank Wen-Li Jia, Dong-Ren Bai, Xiang-Yang Liu, Shu-Bin Zhao, Theresa McCormick, Yi Sun, and Professor Z. H. Lu for their critical contributions to the work described in this Account. The Natural Sciences and Engineering Council of Canada is also greatly acknowledged for financial support.

BIOGRAPHICAL INFORMATION

Zachary M. Hudson was born in 1986 in Ottawa, Ontario. He obtained his B.Sc. in chemistry in 2008 from Queen's University, where he was awarded the Governor General's Medal as the top student at that institution. He joined Suning Wang's research group in 2007 and has been a Canada Graduate Scholar at Queen's since 2008, where he is currently studying organometallic chemistry of triarylboron-containing compounds.

Suning Wang obtained her B.Sc. from Jilin University in China, and her Ph.D. in chemistry from Yale University in Newhaven, CT. In 1986, she joined J.P. Fackler Jr.'s group at Texas A&M University as a postdoctoral fellow. In 1990, she became an assistant professor at the University of Windsor, Ontario, then moved to Queen's University in 1996 where she is now professor, Queen's University research chair, and a recipient of the CSC Alcan award in Inorganic Chemistry. Her research concerns luminescent and supramolecular organometallic materials chemistry.

FOOTNOTES

* To whom correspondence should be addressed. E-mail: suning.wang@chem.queensu.ca.

REFERENCES

- Porres, L.; Charlot, M.; Entwistle, C. D.; Beeby, A.; Marder, T. B.; Blanchard-Desce, M. Novel boron quadrupolar NLO-phores: optimization of TPA/transparency trade-off via molecular engineering. *Proc. SPIE* **2005**, 59340F.
- Entwistle, C. D.; Marder, T. B. Applications of three-coordinate organoboron compounds and polymers in optoelectronics. *Chem. Mater.* **2004**, *16*, 4574–4585.
- Entwistle, C. D.; Marder, T. B. Boron chemistry lights the way: Optical properties of molecular and polymeric systems. *Angew. Chem., Int. Ed.* **2002**, *41*, 2927–2931.
- Yuan, Z.; Collings, J. C.; Taylor, N. J.; Marder, T. B.; Jardin, C.; Halet, J.-F. Linear and nonlinear optical properties of three-coordinate organoboron compounds. *J. Solid State Chem.* **2000**, *154*, 5–12.
- Hudnall, T. W.; Chiu, C. W.; Gabbai, F. P. Fluoride ion recognition by chelating and cationic boranes. *Acc. Chem. Res.* **2009**, *42*, 388–397, and references therein.
- Kim, Y.; Gabbai, F. P. Cationic boranes for the complexation of fluoride ions in water below the 4 ppm maximum contaminant level. *J. Am. Chem. Soc.* **2009**, *131*, 3363–3369.
- Chiu, C. W.; Kim, Y.; Gabbai, F. P. Lewis acidity enhancement of triarylboranes via peripheral decoration with cationic groups. *J. Am. Chem. Soc.* **2009**, *131*, 60–61.
- Yamaguchi, S.; Akiyama, S.; Tamao, K. Colorimetric fluoride ion sensing by boron-containing π -electron systems. *J. Am. Chem. Soc.* **2001**, *123*, 11372–11375.
- Yamaguchi, S.; Wakamiya, A. Boron as a key component for new π -electron materials. *Pure Appl. Chem.* **2006**, *78*, 1413–1424.
- Yamaguchi, S.; Shirasaka, T.; Akiyama, S.; Tamao, K. Dibenzoborole-containing π -electron systems: Remarkable fluorescence change based on the "on/off" control of the $p_{\pi}-\pi^*$ conjugation. *J. Am. Chem. Soc.* **2002**, *124*, 8816–8817.
- Liu, Z.-Q.; Shi, M.; Li, F.-Y.; Fang, Q.; Chen, Z.-H.; Yi, T.; Huang, C. H. Highly selective two-photon chemosensors for fluoride derived from organic boranes. *Org. Lett.* **2005**, *7*, 5481–5484.
- Parab, K.; Venkatasubbaiah, K.; Jäkle, F. Luminescent triarylborane-functionalized polystyrene: Synthesis, photophysical characterization, and anion-binding studies. *J. Am. Chem. Soc.* **2006**, *128*, 12879–12885.
- Jäkle, F. Lewis acidic organoboron polymers. *Coord. Chem. Rev.* **2006**, *250*, 1107–1121.
- Zhou, G.; Baumgarten, M.; Müllen, K. Mesitylboron-substituted ladder-type pentaphenylenes: Charge-transfer, electronic communication, and sensing properties. *J. Am. Chem. Soc.* **2008**, *130*, 12477–12484.
- Welch, G. C.; San Juan, R. R.; Masuda, J. D.; Stephan, D. W. Reversible, metal-free hydrogen activation. *Science* **2006**, *314*, 1124–1126.
- Chase, P. A.; Welch, G. C.; Jurca, T.; Stephan, D. W. Metal-free catalytic hydrogenation. *Angew. Chem., Int. Ed.* **2007**, *46*, 8050–8053.
- Noda, T.; Shirota, Y. 5,5'-Bis-(dimesitylboryl)-2,2'-bithiophene and 5,5'-bis(dimesitylboryl)-2,2':5',2''-terthiophene as a novel family of electron-transporting amorphous molecular materials. *J. Am. Chem. Soc.* **1998**, *120*, 9714–9715.
- Noda, T.; Ogawa, H.; Shirota, Y. A blue-emitting organic electroluminescent device using a novel emitting amorphous molecular material, 5,5'-bis(dimesitylboryl)-2,2'-bithiophene. *Adv. Mater.* **1999**, *11*, 283–285.
- Kinoshita, H.; Okumoto, K.; Shirota, Y. A novel class of emitting amorphous molecular materials with bipolar character for electroluminescence. *Chem. Mater.* **2003**, *15*, 1080–1089.
- Shirota, Y. Organic materials for electronic and optoelectronic devices. *J. Mater. Chem.* **2000**, *10*, 1–25.
- Elbing, M.; Bazan, G. C. A new design strategy for organic optoelectronic materials by lateral boryl substitution. *Angew. Chem., Int. Ed.* **2008**, *47*, 834–838.
- Jia, W.-L.; Feng, X.-D.; Bai, D.-R.; Lu, Z.-H.; Wang, S.; Vamvounis, G. Mes₂B(p-4,4'-biphenyl-NPh(1-naphthyl)): A multifunctional molecule for electroluminescent devices. *Chem. Mater.* **2005**, *17*, 164–170.
- Jia, W.-L.; Moran, M. J.; Yuan, Y.-Y.; Lu, Z.-H.; Wang, S. (1-Naphthyl)phenylamino functionalized three-coordinate organoboron compounds: Syntheses, structures, and applications in OLEDs. *J. Mater. Chem.* **2005**, *15*, 3326–3333.
- Li, F.-H.; Jia, W.-L.; Wang, S.; Zhao, Y.-Q.; Lu, Z.-H. Blue organic light-emitting diodes based on Mes₂B(p-4,4'-biphenyl-NPh(1-naphthyl)). *J. Appl. Phys.* **2008**, *103*, 034509.
- Jia, W.-L.; Song, D.-T.; Wang, S. Blue luminescent three-coordinate organoboron compounds with a 2,2'-dipyridylamino functional group. *J. Org. Chem.* **2003**, *68*, 701–705.
- Jia, W.-L.; Bai, D.-R.; McCormick, T.; Liu, Q.-D.; Motala, M.; Wang, R.-Y.; Seward, C.; Tao, Y.; Wang, S. Three-coordinate organoboron compounds BAr₂R (Ar = mesityl, R = 7-azaindolyl- or 2,2'-dipyridylamino-functionalized aryl or thienyl) for electroluminescent devices and supramolecular assembly. *Chem.—Eur. J.* **2004**, *10*, 994–1006.
- Zhao, S.-B.; Wucher, P.; Hudson, Z. M.; McCormick, T. M.; Liu, X.-Y.; Wang, S.; Feng, X.-D.; Lu, Z.-H. Impact of the linker on electronic and luminescent properties of diboryl compounds: Molecules with two BMes₂ groups and the peculiar behavior of 1,6-(BMes₂)₂pyrene. *Organometallics* **2008**, *27*, 6446–6456.
- Liu, X.-Y.; Bai, D.-R.; Wang, S. Charge-transfer emission in nonplanar three-coordinate organoboron compounds for fluorescent sensing of fluoride. *Angew. Chem., Int. Ed.* **2006**, *45*, 5475–5478.
- Bai, D.-R.; Liu, X.-Y.; Wang, S. Charge-transfer emission involving three-coordinate organoboron: V-shape versus U-shape and impact of the spacer on dual emission and fluorescent sensing. *Chem.—Eur. J.* **2007**, *13*, 5713–5723.
- Sun, Y.; Ross, N.; Zhao, S.-B.; Huszarik, K.; Jia, W.-L.; Wang, R.-Y.; Wang, S. Enhancing electron accepting ability of triarylboron via π -conjugation with 2,2'-Bipy and metal chelation: 5,5'-Bis(BMes₂)-2,2'-bipy and its metal complexes. *J. Am. Chem. Soc.* **2007**, *129*, 7510–7511.
- Sun, Y.; Wang, S. Conjugated triarylboron donor-acceptor systems supported by 2,2'-bipyridine: Metal chelation impact on intra-ligand charge transfer emission, electron accepting ability and "turn-on" fluoride sensing. *Inorg. Chem.* **2009**, *48*, 3755–3767.
- Zhao, S.-B.; McCormick, T.; Wang, S. Ambient-temperature metal-to-ligand charge-transfer phosphorescence facilitated by triarylboron: Bnpa and its metal complexes. *Inorg. Chem.* **2007**, *46*, 10965–10967.
- Hudson, Z. M.; Zhao, S.-B.; Wang, R.-Y.; Wang, S. Switchable Ambient-Temperature Singlet-Triplet Dual Emission in Nonconjugated Donor-Acceptor Triarylboron-Pt(II) Complexes. *Chem.—Eur. J.* **2009**, *15*, 6131–6137.
- Liu, Q. D.; Mudadu, M. S.; Thummel, R.; Tao, Y.; Wang, S. From blue to red: Syntheses, structures, electronic, and electroluminescent properties of tunable luminescent N,N-chelate boron complexes. *Adv. Funct. Mater.* **2005**, *15*, 143–154.
- Liu, S. F.; Wu, Q.; Schmider, H. L.; Aziz, H.; Hu, N. X.; Popovic, Z.; Wang, S. Syntheses, structures, and electroluminescence of new blue/green luminescent chelate compounds: Zn(2-py-in)₂(THF), BPh₂(2-py-in), Be(2-py-in)₂, and BPh₂(2-py-aza) [2-py-in = 2-(2-pyridyl)indole; 2-py-aza = 2-(2-pyridyl)-7-azaindole]. *J. Am. Chem. Soc.* **2000**, *122*, 3671–3678.
- Wu, Q.; Esteghamatian, M.; Hu, N. X.; Popovic, Z.; Enright, G.; Breeze, S. R.; Wang, S. Isomerism and blue electroluminescence of a novel organoboron compound: B₂(O)(7-azaindyl)₂Ph₂. *Angew. Chem., Int. Ed.* **1999**, *38*, 985–988.
- Wang, S. Luminescence and electroluminescence of Al(III), B(III), Be(II) and Zn(II) complexes with nitrogen donors. *Coord. Chem. Rev.* **2001**, *215*, 79–98.
- Zhao, S. B.; Wang, R. Y.; Wang, S. Intramolecular C–H activation directed self-assembly of an organoplatinum(II) molecular square. *J. Am. Chem. Soc.* **2007**, *129*, 3092–3093.
- Schulz, A.; Kaim, W. Organoboron redox systems. *Chem. Ber.* **1989**, *122*, 1863–1868.
- Melaimi, M.; Gabbai, F. P. A heteronuclear bidentate Lewis acid as a phosphorescent fluoride sensor. *J. Am. Chem. Soc.* **2005**, *127*, 9680–9681.

- 41 Sakuda, E.; Funahashi, A.; Kitamura, N. Synthesis and spectroscopic properties of platinum(II) terpyridine complexes having an arylborane charge transfer unit. *Inorg. Chem.* **2006**, *45*, 10670–10677.
- 42 Zhou, G. J.; Ho, C. L.; Wong, W. Y.; Wang, Q.; Ma, D. G.; Wang, L. X.; Lin, Z. Y.; Marder, T. B.; Beeby, A. Manipulating charge-transfer character with electron-withdrawing main-group moieties for the color tuning of iridium electrophosphors. *Adv. Funct. Mater.* **2008**, *18*, 499–511.
- 43 You, Y. M.; Park, S. Y. A phosphorescent Ir(III) complex for selective fluoride ion sensing with a high signal-to-noise ratio. *Adv. Mater.* **2008**, *20*, 3820–3826.
- 44 Zhao, Q.; Li, F. Y.; Liu, S. J.; Yu, M. X.; Liu, Z. Q.; Yi, T.; Huang, C. H. Highly selective phosphorescent chemosensor for fluoride based on an iridium(III) complex containing arylborane units. *Inorg. Chem.* **2008**, *47*, 9256–9264.